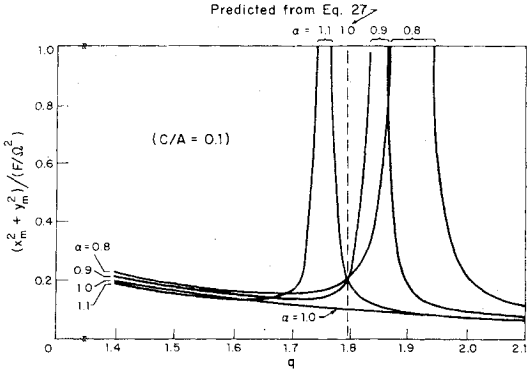

Fig. 2 Dedamper response vs frequency ratio.

could be constructed with precisely equal spring constants in the two directions, then the Coriolis forces acting during vibration would suppress the resonance in a spacecraft for which $C<A$. However, if the spring constants are even slightly different, then this interaction with Coriolis forces is not perfect and a resonant condition indeed occurs. This behavior is illustrated graphically by examining a combined response parameter vs frequency as determined by digital computer simulation of the complete, linearized equations-of-motion (Fig. 2). At $\alpha=1$, the sharp resonance is indeed suppressed, which could lead an unwary analyst to conclude that such a system has no resonance and therefore poses no problems with regard to dedamping or excessive structural deflections. This phenomenon is just one more example of a situation in spin-stabilized satellite dynamics in which treating an apparently simple case can lead to erroneous conclusions.

Conclusions

A two-DOF system mounted on a spin-stabilized spacecraft and whose motion is in a plane normal to the spin-axis exhibits the phenomenon of "frequency splitting," which results in its possessing two natural frequencies. However, only one of the frequencies can be in resonance with the nutation rate on any specific spacecraft.

References

[1]Fang, B. T., "Kinetic Energy and Angular Momentum about the Variable Center of Mass of a Satellite," *AIAA Journal*, Vol. 3, Aug. 1965, pp. 1540-1542.

[2]Cloutier, G. J., "Variable Spin-Rate Two-Degrees-of-Freedom Nutation Damper Dynamics," AAS/AIAA Astrodynamics Conference, July 28-30, 1975.

[3]Likins, P. W., Barbera, F. J., and Baddeley, V., "Mathematical Modeling of Spinning Elastic Bodies for Modal Analysis," *AIAA Journal*, Vol. 11, Sept. 1973, pp. 1251-1258.

[4]Cloutier, G. J., "Optimum Design Parameters for a Spin-Stabilized Spacecraft Nutation Damper," *Journal of Spacecraft and Rockets*, Vol. 9, June 1972, pp. 466-468.

Effect of Nozzle Submergence upon Stability of Solid Rockets

B.A. Janardan* and B.T. Zinn†
Georgia Institute of Technology, Atlanta, Ga.

THE linear stability of a solid propellant rocket combustor is generally determined by evaluating the rate of growth or decay of a small-amplitude oscillation inside the combustor. A common representation of the behavior of the combustor pressure disturbance, in terms of a net growth-decay coefficient α_{gd}, is

$$p_1(z,t) = P(z)e^{\alpha_{gd}t}e^{i\omega t} \tag{1}$$

In this representation, the growth or decay of the disturbance is determined by the sign of the coefficient α_{gd}. It can be shown,[1] that α_{gd} can be expressed as

$$\alpha_{gd} = \sum_i \alpha_i$$

where the components α_i describe the contributions of the various relevant engine processes (e.g., combustion process, nozzle, etc.) to motor stability. Consequently, the effect of any particular process upon engine stability may be evaluated by investigating the manner in which the α_i which pertains to the process under consideration depends upon relevant engine design parameters. This Note is concerned with the determination of the dependence of nozzle damping, described by the nozzle decay coefficient α_N, upon the nozzle submergence into the combustor of a solid rocket. This investigation has been motivated by experimental evidence[2] indicating that the submergence of a nozzle into the combustor resulted in a transition from a stable to an unstable operation in an experimental engine. Since submerged nozzles are currently in use in solid rocket motors, it is of importance to develop an understanding of the causes of such a behavior so that it would not occur in future rocket motors.

In a typical application, as shown in Fig. 1, a submerged nozzle is recessed into the combustion chamber where it is surrounded by the solid propellant grain. After ignition, the regression of the burning propellant surface results in an increase with time of both the depth of the cavity surrounding the nozzle and the flow rate of combustion products from the cavity into the main chamber. The effect of the nozzle cavity depth and the flow rate issuing from the cavity of a typical submerged nozzle configuration upon the nozzle admittance has been experimentally investigated.[3] It is the objective of this Note to determine the characteristics of the decay coefficient for the submerged nozzle from the measured nozzle admittance data. The following discussion will demonstrate the necessity to take into consideration the "reversed" cavity flow at the nozzle entrance plane while computing α_N for a combustor with a submerged nozzle.

The growth or decay rate of a small amplitude oscillation in a cavity with mean flow has been considered in detail by Cantrell and Hart.[4] Using the mass, momentum, and energy conservation laws, and assuming that all wave-energy addition or removal occurs at the cavity's boundaries, they derived an expression that relates the growth or decay rate of the chamber oscillation to the conditions at the cavity's boundaries. In the evaluation of the nozzle decay coefficient α_N, it is customarily assumed that the nozzle is the only wave-energy loss mechanism present in the system. Under these conditions, the surface integration indicated in the Cantrell and Hart result is to be performed over the nozzle entrance area only. In this situation, the Cantrell and Hart expression for α_N reduces to the following form.[3]

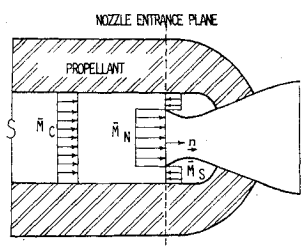

Fig. 1 Schematic representation of a submerged rocket nozzle. Chamber cross-sectional area $=S_C$; cavity entrance area $=S_S$; nozzle entrance area $=S_N$.

Received July 8, 1975; revision received September 11, 1975. This research was supported by Air Force Rocket Propulsion Laboratory, Edwards, California, under contract F04611-71-C-0054.

Index categories: Combustion Stability, Ignition, and Detonation; Solid and Hybrid Rocket Engines.

*Research Engineer, School of Aerospace Engineering.

†Regents' Professor of Aerospace Engineering. Associate Fellow AIAA.

$$2\alpha_N \hat{V} = -\left\langle \int_{\text{nozzle entrance}} d\mathbf{S}\boldsymbol{n}\cdot\{p_1\boldsymbol{u}_1 + \frac{\bar{M}}{\bar{\rho}\bar{c}}p_1^2 + \bar{\rho}\bar{c}(\bar{\boldsymbol{M}}\cdot\boldsymbol{u}_1)\boldsymbol{u}_1 + (\bar{\boldsymbol{M}}\cdot\boldsymbol{u}_1)p_1\bar{\boldsymbol{M}}\}\right\rangle \quad (2)$$

where

$$\hat{V} = \left\langle \int_{\text{combustor volume}} dV\{\tfrac{1}{2}\bar{\rho}\boldsymbol{u}_1\cdot\boldsymbol{u}_1 + \tfrac{1}{2}\frac{p_1^2}{\bar{\rho}\bar{c}^2} + \frac{\bar{\boldsymbol{M}}\cdot\boldsymbol{u}_1}{\bar{c}}p_1\}\right\rangle \quad (3)$$

and $\boldsymbol{n}$ is a unit normal vector pointing out of the combustor. The notation $\langle\ \rangle$ is employed here to denote time averaging. An examination of Eqs. (2) and (3) indicates that the acoustic mode structure (i.e., the pressure perturbation p_1 and the velocity perturbation $\boldsymbol{u}_1$) and the steady-state flow properties such as the Mach number $\bar{M}$, density $\bar{\rho}$, and the velocity of sound $\bar{c}$ must be known for the evaluation of α_N.

To determine the attenuation of a disturbance in a combustor with a submerged nozzle, the flow behavior in such a combustor is approximated in this investigation by the velocity profiles shown in Fig. 1. In this figure, $\bar{M}_N$ represents the effective mean flow Mach number entering the nozzle, $\bar{M}_S$ represents the effective mean flow Mach number of the flow leaving the cavity and entering the main chamber, and $\bar{M}_C$ represents the effective mean flow Mach number of the primary flow in the chamber. The magnitude of the nozzle effective mean flow Mach number $\bar{M}_N$ is chosen to satisfy the steady-state mass conservation equation for the flow configuration shown in Fig. 1. Recognizing that this steady-state flow representation is at best only an approximation and assuming that the oscillations in the combustor are one-dimensional, the application of Eq. (2) to the flow representation shown in Fig. 1 results in the following expression for α_N

$$2\alpha_N \hat{V} = -[(S_C + \bar{M}_N^2 S_N + \bar{M}_S^2 S_S)\langle p_1 u_1\rangle + (\bar{M}_N S_N - \bar{M}_S S_S)\left(\frac{\langle p_1^2\rangle}{\bar{\rho}\bar{c}} + \bar{\rho}\bar{c}\langle u_1^2\rangle\right)] \quad (4)$$

In deriving Eq. (4) the relationships $\bar{\boldsymbol{M}}_N\cdot\boldsymbol{n} = \bar{M}_N$, $\bar{\boldsymbol{M}}_S\cdot\boldsymbol{n} = -\bar{M}_S$ and $\boldsymbol{u}_1\cdot\boldsymbol{n} = u_1$ have been used. To evaluate the volume integral, defined in Eq. (3), the reverse flow in that part of the chamber near the cavity entrance is neglected and for a one-dimensional oscillation Eq. (3) reduces to

$$\hat{V} = S_C\left\langle \int_0^{L_C}\left[\frac{\bar{\rho}}{2}u_1^2 + \frac{1}{2\bar{\rho}\bar{c}^2}p_1^2 + \frac{\bar{M}_C}{\bar{c}}u_1 p_1\right] dz\right\rangle \quad (5)$$

where L_C is the chamber length.

The time and space integrations indicated in Eqs. (4) and (5) can be performed only if the time dependence and mode structure of the oscillations inside the combustor are known. The required expressions are obtained[5] by solving the system of conservation equations that describe the behavior of small-amplitude, one-dimensional disturbances that are superimposed upon a steady one-dimensional flow inside a simulated rocket combustor. These acoustic solutions are then required to satisfy the admittance boundary condition at the nozzle entrance plane. The resulting expressions describing the time and space dependence of the pressure and velocity perturbations inside the simulated combustor are:[3,5]

$$p_1(z,t) = \gamma\bar{p}\hat{A}e^{i(\omega t + az)}\cosh(\Phi - iRz) \quad (6)$$

$$u_1(z,t) = \bar{c}\hat{A}e^{i(\omega t + az)}\sinh(\Phi - iRz) \quad (7)$$

where

$$\Phi = \pi\alpha - i\pi[\beta + 2(L_C - z)/\lambda + \tfrac{1}{2}] \quad (8)$$

$$R = \frac{\omega/\bar{c}}{(1-\bar{M}^2)};\ a = R\bar{M};\ \lambda = \frac{2\pi}{R} \quad (9)$$

and $\hat{A}$ = constant. The parameters α and β that appear in Eq. (8), respectively, describe the changes in amplitude and phase between the reflected and incident pressure waves at the nozzle entrance plane. In addition, they describe the admittance y_N at the nozzle entrance plane as evident from the following relationship[3,5]

$$y_N = \frac{u_1}{p_1}\bar{\rho}\bar{c} = \coth\pi(\alpha - i\beta) \quad (10)$$

where $1/\bar{\rho}\bar{c}$ is the characteristic admittance of the gas medium at the nozzle entrance.

Substituting Eqs. (6) and (7) into Eqs. (4) and (5) and performing the indicated space and time integrations, the following expression for the nondimensional nozzle decay coefficient, Λ_N, for a combustor with a submerged nozzle is obtained

$$\Lambda_N = \frac{\alpha_N L_C}{\bar{c}} = -\frac{(\bar{M}_N\sigma_N - \bar{M}_S\sigma_S) + [(1 + \bar{M}_N^2\sigma_N + \bar{M}_S^2\sigma_S)/2]\tanh(2\pi\alpha)}{[1 + \bar{M}_C\tanh(2\pi\alpha)]} \quad (11)$$

where $\sigma_N = S_N/S_C$ is the nozzle open-area ratio and $\sigma_s = S_S/S_C = (1-\sigma_N)$ is the cavity open-area ratio. An examination of Eq. (11) indicates that for the case under consideration, the nondimensional decay coefficient of a submerged nozzle is a function only of the mean flow Mach numbers $\bar{M}_N$, $\bar{M}_S$, and $\bar{M}_C$, the open-area ratio σ_S of the cavity and the admittance parameter α which describes the "average" amplitude attenuation provided at the nozzle entrance plane. When no cavity flow is present in the system (i.e., $\bar{M}_S = 0$) Eq. (11) reduces to

$$\Lambda_N = \frac{\bar{M}_N\sigma_N + [(1 + \bar{M}^2{}_N\sigma_N)/2]\tanh(2\pi\alpha)}{[1 + \bar{M}_C\tanh(2\pi\alpha)]} \quad (12)$$

A comparison of Eq. (11) with Eq. (12) indicates that the presence of a cavity "reverse" flow added two terms to Eq. (12). The first of these terms, namely $\bar{M}_S\sigma_S$, results in a decrease in nozzle damping while the second term $-\frac{1}{2}\bar{M}_S^2\sigma_S\tanh(2\pi\alpha)$ results in an increase in nozzle damping. However, from an order of magnitude consideration, it is evident that the first term is larger than the second term. Hence, it can be observed that the presence of the "reverse cavity" flow reduces nozzle damping and thus decreases engine stability.

To illustrate the application of Eq. (11), the characteristics of the decay coefficient of the submerged nozzle configuration tested in Ref. 3 have been calculated. The test configuration of Ref. 3 had a short submerged nozzle and the admittance boundary conditions at the nozzle entrance plane were determined with $\bar{M}_N = 0.08$ and the cavity-to-chamber flow rate ratio varying between zero and 25% in steps of 5%. The cavity depth was also varied from zero to 24 in. beyond the nozzle entrance plane (i.e., see Fig. 5 of Ref. 3 for details). The admittance of the submerged nozzle configuration was measured using the modified impedance tube technique. An examination of the measured admittance data (see Ref. 3) indicate that both the cavity depth and the cavity flow rate have a negligible effect upon the measured value of the parameter α. Using the available experimental data together with Eq. (11), one is led to the conclusion that for a given cavity flow rate (i.e., given $\bar{M}_S$) the cavity depth has a negligible effect

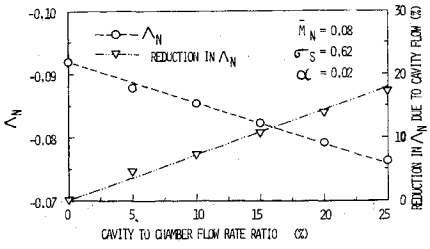

Fig. 2 Effect of cavity flow on the decay coefficient of submerged nozzle configuration of Ref. 3.

upon the nozzle decay coefficient Λ_N. However, for a given cavity depth, it can be observed that the nozzle decay coefficient Λ_N depends upon the cavity Mach number $\bar{M}_S$, and hence upon the cavity flow rate. To illustrate this dependence, the magnitude of Λ_N for the submerged nozzle configuration studied in Ref. 3 has been computed and the data are presented in Fig. 2. Also presented in this figure is the percent reduction in the value of Λ_N with increase in cavity flow when compared with no cavity flow in the test configuration. An examination of this figure indicates that, for example, when the cavity-to-chamber flow rate ratio is increased from 0 to 15%, a 10% reduction in Λ_N is observed. Suppose a given rocket motor, when using the nozzle under consideration without submergence was found to be marginally stable, then submerging this nozzle into the rocket combustor would undoubtedly result in a transition from stability to instability, due to the reduction in the effective nozzle damping.

The main conclusion that follows from this study on submerged nozzles is that the presence of the "reverse" cavity flow reduces the effective nozzle damping. This reduction in the damping capability of the nozzle offers one possible explanation to the observed[2] decrease in the stability of an experimental solid rocket motor when the nozzle was submerged into the combustor.

References

[1] Coates, R.L. and Horton, M.D., "Design Considerations for Combustion Instability," *Journal of Spacecraft and Rockets,* Vol. 6, March 1969, pp. 296-302.

[2] Micheli, P., private communication.

[3] Janardan, B.A., Daniel, B.R., and Zinn, B.T., "Damping of Axial Instabilities by Small-Scale Nozzles under Cold-Flow Conditions," *Journal of Spacecraft and Rockets,* Vol. 11, Dec. 1974, pp. 812-820.

[4] Cantrell, R.A. and Hart, R.W., "Interaction Between Sound and Flow in Acoustic Cavities; Mass, Momentum and Energy Considerations," *The Journal of the Acoustic Society of America,* Vol. 36, April 1964, pp. 697-706.

[5] Zinn, B.T., Bell, W.A., Daniel, B.R., and Smith, A.J., Jr., "Experimental Determination of Three-Dimensional Liquid Rocket Nozzle Admittances," *AIAA Journal,* Vol. 11, March 1973, pp. 267-272.

Solution Bounds to Structural Systems

V. R. Murthy* and T. J. McDaniel†
Iowa State University, Ames, Iowa

I. Introduction

THE theory of differential and integral inequalities provides a method of constructing bounds to the solution for a wide range of engineering problems. The texts of Walter,[1] Protter and Weinberger,[2] and Lakshmikantham and Leela[3] summarize the major theorems and contain numerous references. In theory it is possible to construct both upper and lower bounds to the solution for certain classes of partial differential equations and to systems of ordinary differential and integral equations. In practice it is not a simple matter to construct such bounds.

In the present Note a procedure is sought which directly yields such bounds for an arbitrary system of variable coefficient linear differential equations, such that upper and lower bounds agree to a prescribed number of digits. An efficient means of refining these bounds is then required. To illustrate the procedures which are developed, bounds on the buckling load and the buckling shape of a varying geometry column will be obtained.

The theory of differential and integral inequalities applies primarily to initial value problems. Since the transfer matrix method, which has been applied to a variety of engineering problems,[4-6] converts a two point boundary value problem to an initial value problem, the inequality theorems directly apply to linear structures with varying geometry. The inequality theorems have not been developed sufficiently to allow the construction of bounds to two point nonlinear boundary value problems except for special classes of problems.

It is evident from the literature that few engineering applications of the inequality theorems have been carried out. This is partially due to a lack of direct procedures for constructing such bounds. Also, one may suspect that the extra computational effort involved in producing such bounds does not justify the convenience of having such bounds. Actually, the generation of bounds can lead to computational efficiency, which is obtained by using limited accuracy intermediate computations. The accuracy of the final computation can be judged by the number of places of agreement of the upper and lower bounds of that solution.

Some applications of the theory of inequalities to boundary-layer flow,[7-8] flow of viscous fluid in a narrow slit,[9] and heat conduction,[10] have been accomplished. In general, high precision in the results was not demonstrated. In more recent articles[11,12] quite accurate bounds have been obtained by using differential inequalities. Reference 11 computed upper and lower bounds to the response of a nonlinear single degree-of-freedom system which gave good agreement of the bounds (7 or more digits) over the range of computation. This approach does require considerable computation to obtain the required bounds. Reference 12 avoids this difficulty for a specialized system of differential equations associated with the analysis of beams with varying geometry. Rough analytical bounds were improved by Picard iteration to obtain good agreement (4 or 5 digits) between the upper and lower bounds for the required transfer matrix elements. Both upper and lower bounds on the transfer matrix were computed in less time than required for a standard Runge-Kutta procedure to obtain a numerical transfer matrix. Bounds on the solution state vector were also in agreement to 3 or 4 places. We hope to demonstrate the same computational efficiency in obtaining bounds for a more general system of equations considered following.

II. Application of Differential Inequalities

Consider a variable coefficient linear differential equation of the type

$$d/dx[T(x)] = [A(x)]\,[T(x)] \qquad 0 \le x \le \ell \tag{1}$$

with initial conditions $[T(0)] = [I]$ (2)

The desired solution to the previous equation is the transfer matrix $[T(x)]$. $[T(x)]$ exists and is unique if the elements of $[A(x)]$ are piecewise continuous and bounded. The elements

Received May 7, 1975; revision received September 19, 1975. This research was sponsored by the National Science Foundation under Grant GK-40589 and by the Iowa State University Engineering Research Institute.

Index category: Structural Stability Analysis.

*Research Assistant Professor of Aerospace Engineering and Engineering Research Institute.

†Associate Professor of Aerospace Engineering and Engineering Research Institute. Member AIAA.